ASN NEURO RESEARCH ARTICLE

Supplementary data

ASN NEURO 4(1):art:e00073.doi:10.1042/AN20110037

Altered synaptic marker abundance in the hippocampal stratum oriens of Ts65Dn mice is associated with exuberant expression of versican

Matthew D Howell and Paul E Gottschall[1]
Department of Pharmacology and Toxicology, University of Arkansas for Medical Sciences, Little Rock, AR 72205, U.S.A.

Cite this article as: Howell, MD and Gottschall, PE (2012) Altered synaptic marker abundance in the hippocampal stratum oriens of Ts65Dn mice is associated with exuberant expression of versican. ASN NEURO 4(1):art:e00073.doi:10.1042/AN20110037

ABSTRACT

DS (Down syndrome), resulting from trisomy of chromosome 21, is the most common cause of genetic mental retardation; however, the molecular mechanisms underlying the cognitive deficits are poorly understood. Growing data indicate that changes in abundance or type of CSPGs (chondroitin sulfate proteoglycans) in the ECM (extracellular matrix) can influence synaptic structure and plasticity. The purpose of this study was to identify changes in synaptic structure in the hippocampus in a model of DS, the Ts65Dn mouse, and to determine the relationship to proteoglycan abundance and/or cleavage and cognitive disability. We measured synaptic proteins by ELISA and changes in lectican expression and processing in the hippocampus of young and old Ts65Dn mice and LMCs (littermate controls). In young (5 months old) Ts65Dn hippocampal extracts, we found a significant increase in the postsynaptic protein PSD-95 (postsynaptic density 95) compared with LMCs. In aged (20 months old) Ts65Dn hippocampus, this increase was localized to hippocampal stratum oriens extracts compared with LMCs. Aged Ts65Dn mice exhibited impaired hippocampal-dependent spatial learning and memory in the RAWM (radial-arm water maze) and a marked increase in levels of the lectican versican V2 in stratum oriens that correlated with the number of errors made in the final RAWM block. Ts65Dn stratum oriens PNNs (perineuronal nets), an extension of the ECM enveloping mostly inhibitory interneurons, were dispersed over a larger area compared with LMC mice. Taken together, these data suggest a possible association with alterations in the ECM and inhibitory neurotransmission in the Ts65Dn hippocampus which could contribute to cognitive deficits.

Key words: chondroitin sulfate proteoglycan, Down syndrome, extracellular matrix, stratum oriens, Ts65Dn, versican.

INTRODUCTION

DS (Down syndrome) results from trisomy of human chromosome 21 and is the most common genetic cause of mental retardation (Canfield et al., 2006). The neurological phenotype of DS patients may range from severe cognitive dysfunction to milder learning impairments (Epstein, 2002), and nearly all DS subjects exhibit AD (Alzheimer's disease) pathology by the fourth decade of life (Burger and Vogel, 1973). The detailed molecular mechanism(s) that lead(s) to cognitive deficits either in young or older DS subjects is poorly understood. Studies have demonstrated changes in synaptic structure in key cognitive brain regions, including the hippocampus, and suggest that these contribute to mental retardation (Belichenko et al., 2004, 2007; Popov et al., 2011).

The most widely used research model of DS, the Ts65Dn mouse (Davisson et al., 1990; Reeves et al., 1995) takes advantage of synteny between a large portion of mouse chromosome 16 and human chromosome 21. A segment of mouse chromosome 16 is translocated on to chromosome 17 which results in triplication of about half the genes that are

[1]To whom correspondence should be addressed (email pegottschall@uams.edu).

Abbreviations: ADAMTS, a distintegrin and metalloproteinase with thrombospondin motifs; BCA, bicinchoninic acid; CNS, central nervous system; CSPG, chondroitin sulfate proteoglycan; C_t, threshold cycle value; DS, Down syndrome; DSCR, Down syndrome critical region; ECM, extracellular matrix; GABA, γ-aminobutyric acid; GAPDH, glyceraldehyde-3-phosphate dehydrogenase; GFAP, glial fibrillary acidic protein; HRP, horseradish peroxidase; OCT, optimal cutting temperature; PNN, perineuronal net; RAWM, radial-arm water maze; LMC, littermate control; LTP, long-term potentiation; PSD-95, postsynaptic density 95; qRT–PCR, quantitative reverse transcription–PCR; SNAP-25, 25 kDa synaptosome-associated protein; WFA, *Wisteria floribunda* agglutinin.

triplicated in DS (Olson et al., 2004). Neurologically, in the Ts65Dn hippocampus, there are abnormally sized presynaptic terminals, enlarged dendritic spines, altered inhibitory and excitatory circuitry (Belichenko et al., 2004, 2007, 2009b), deficits in LTP (long-term potentiation) (Siarey et al., 1997, 1999; Kleschevnikov et al., 2004), and reduced hippocampal-dependent learning and memory (Demas et al., 1996, 1998; Escorihuela et al., 1998; Hyde et al., 2001; Hunter et al., 2003). A region of human chromosome 21 termed the DSCR (Down syndrome critical region) is triplicated in Ts65Dn, and this region has been hypothesized to be sufficient to cause the DS phenotype. In fact, a mouse model with triplication of just the DSCR genes exhibited a neurobiological phenotype characteristic of DS (Belichenko et al., 2009a). Recent gene expression studies have revealed a chromosome 21 gene, *Adamts1* (a disintegrin and metalloproteinase with thrombospondin motifs-1), was up-regulated 3.7-fold in DS prefrontal cortex (46-76 years old) when compared with control brains, well beyond the predicted 1.5-fold increase expected due to gene dosage (Lockstone et al., 2007). Interestingly, no change in *Adamts1* expression was seen in fetal DS brain, suggesting an age-related effect. *Adamts5*, another chromosome 21 gene, is also triplicated in DS. Studies with human DS subjects have shown an age-related decline of cognitive function (Thase et al., 1984) perhaps implicating an age-related dysregulation of *Adamts1* that could be involved in the cognitive deficits.

ADAMTS1 is one of several members of the secreted ADAMTS metalloproteinase family capable of cleaving the core protein of a small subset of CSPGs (chondroitin sulfate proteoglycans), termed lecticans (Jones and Riley, 2005; Porter et al., 2005). Lecticans are a major component of the ECM (extracellular matrix) in the CNS (central nervous system) (Yamaguchi, 2000; Rauch, 2007) that, together with hyaluronic acid and smaller glycoproteins, form an aggregate lattice in the extracellular space. This aggregate encompasses neurons as PNNs (perineuronal nets) (Bruckner et al., 1993) and also surrounds synapses. Functionally, CSPGs have been shown to be inhibitory towards neurite outgrowth (Galtrey and Fawcett, 2007; Zimmermann and Dours-Zimmermann, 2008). Data from our laboratory indicated that cleavage of the lecticans by the ADAMTSs loosens the ECM aggregate and promotes a more neuroplastic microenvironment. Indeed, we have shown that the ADAMTSs enhance neurite outgrowth *in vitro* (Hamel et al., 2008) and are selectively active in brain regions showing terminal sprouting in models of plasticity (Yuan et al., 2002; Mayer et al., 2005). Thus, increased ADAMTS1 in the Ts65Dn brain could lead to dysfunctional alterations in the ECM. Altered cleavage of lecticans, however, may not be the only contributor to the structural and functional deficits. A change in the deposition of the matrix component reelin, for example, was shown to be involved in the loss of cognitive processes in the aged Ts65Dn hippocampus (Kern et al., 2011). This finding suggests that there may also be changes in the abundance of matrix molecules such as the lecticans that could affect neuronal structure as well as cognition. The accumulation of reelin (and tau in the extracellular space) was seen in aged Ts65Dn mice and has also been noted to occur to a greater extent in untreated aged mice (Kuo et al., 1996; Mitsuno et al., 1999).

Since changes in the ECM aggregate can affect synapse maintenance and development and since marked overexpression of *Adamts1* was seen in adult DS prefrontal cortex, the aim of this study was to determine whether alterations in processing of lecticans in brain ECM due to abnormal expression of ADAMTS1 in the Ts65Dn mouse was associated with changes in synaptic abundance. Our studies examined both adult (5 months old) and aged (20 months old) mice for several reasons. The loss of basal forebrain cholinergic neurons, the major cholinergic input to the hippocampus, occurs after 5 months of age (Cooper et al., 2001) and has been postulated to be involved with cognitive deficits in DS patients and the Ts65Dn mouse (Isacson et al., 2002). Basal forebrain cholinergic neurons continue to degenerate with aging (Holtzman et al., 1996; Cooper et al., 2001), and several studies have shown that cognitive deficits become more severe with aging in DS patients (Thase et al., 1984; Nelson et al., 2005) and in the Ts65Dn mouse (Holtzman et al., 1996; Kurt et al., 2000; Salehi et al., 2009). Given the increased expression of *Adamts1* in aged DS patients and an increase in extracellular granules seen in aged Ts65Dn mice, it is possible that changes in ECM processing and abundance could become more apparent in the aged mouse.

We have developed several ELISAs to measure protein markers of synapses (Gottschall et al., 2010), and these markers are thought to reflect the abundance of synapses. There are conflicting reports in the literature as to whether synaptic proteins are altered in the brain of Ts65Dn mice. Synaptophysin was reported to be significantly decreased in adult Ts65Dn hippocampus (Pollonini et al., 2008), yet synaptophysin levels were unchanged in whole brain synaptosomal preparations (Fernandez et al., 2009). However, these synaptic marker levels in these studies were measured by immunoblot which is less quantitative than ELISA. In this study, ELISA measurement of synaptic marker proteins was used to examine whether there are changes in synaptic abundance in Ts65Dn brain regions and whether they are associated with ADAMTS1-derived changes in lectican processing.

MATERIALS AND METHODS

Animals

All animal protocols were approved by the Institutional Animal Care and Use Committee at the University of Arkansas for Medical Sciences and every effort was made to limit the number of animals required for these experiments. Male Ts65Dn and LMC (littermate control) mice were purchased from the Jackson Laboratory (stock 001924). Mice were housed individually under standard laboratory conditions with access to food and water *ad libitum*. Mice were aged

until 5 or 20 months before behavioural testing and/or killing. All behavioural testing was performed during the light phase of the 12 h light/12 h dark cycle. Seven LMC and eight Ts65Dn mice at five months of age and 11 LMC and nine Ts65Dn mice at 20 months of age were subjects in these experiments.

RAWM (radial-arm water maze)

To examine spatial cue recognition learning and memory in LMC and Ts65Dn mice, we utilized a modified version of the RAWM (Alamed et al., 2006). Twenty-month-old Ts65Dn (n=9) and LMC (n=11) mice were randomly assigned a number and divided into two separate cohorts that were tested at different times. All mice were housed separately and the experimenter was blinded to the genotype. The RAWM consisted of a wading pool (89 cm wide and 19 cm high) spray painted black with a metal insert (84 cm wide and 14 cm high) that divided the pool into six equal lanes. Each mouse was randomly assigned a goal arm where the platform was placed for every trial. The start arm was randomly chosen and varied for each mouse for each trial. Spatial cues were simple geometric shapes (triangle, diamond and rectangle) that were clipped around the pool and remained in the same spot for all trials. The experimenter was also a visual cue and remained in the same spot for all trials for all mice. The water in the pool was maintained at 20°C.

On day 1 the mice were trained on the RAWM. Two groups of six mice separately received 12 trials. For the first trial, a mouse was released from the start arm and had 60 s to find a visible platform in the goal arm. An error was considered as either an entry into an arm without the platform or 15 s without entering an arm or remaining in an incorrect arm. If the mouse did not locate the platform after 60 s it was gently guided to it; all mice remained on the platform for 10 s. For the second trial, the platform was switched to hidden (an all black terracotta pot hidden 2 mm below the water surface) but was otherwise identical with the first trial. The third trial used the visible platform as in trial 1. The fourth to sixth trials used the hidden platform. After six trials the first cohort rested under heat lamps while the second cohort received trials 1–6 as described above. The first cohort then received six additional trials with only the hidden platform and this protocol was repeated for the second cohort. The mice were tested again on day 2 to determine their ability to recall the location of the platform based on the spatial cues. Day 2 testing proceeded as on day 1, except the hidden platform was used for all trials. The mice were then tested 1 week later (day 9) following the same protocol as for day 2. The average number of errors a mouse made over a block of three trials (block 1 was trials one through three, block 2 was trials four to six, etc.) was calculated and used for analysis. We excluded four LMC mice from analysis due to lack of active learning during the RAWM – they would avoid climbing on the platform and continue swimming in the pool. When examining the correlation with the Ts65Dn stratum oriens, one value was excluded from analysis. This sample had high versican V2 abundance but a low number of errors for only the final block of the RAWM.

Tissue preparation

Mice were killed with an overdose of carbon dioxide and the brain removed from the skull. For some mice the brain was cut sagitally and half was placed in 4% (w/v) PFA (paraformaldehyde) overnight and then placed in PBS containing 0.04% sodium azide until processed further for immunohistochemistry. Cerebellum, brainstem, frontal cortex, temporal cortex, hippocampus, rest of cortex and rest of brain were dissected from the other half and stored at −80°C until use. For some brains, the cerebellum and frontal cortex were removed and the remainder of the brain was flash frozen in dry-ice cooled hexane (Sigma–Aldrich) for 15 s, and then stored in a freezer at −80°C for hippocampal microdissection (see below).

Protein was extracted from brain regions using RIPA buffer [50 mM Tris/HCl, 150 mM NaCl, 2 mM EDTA, 1% DOC (sodium deoxycholate), 0.1% SDS and 1% Triton X-100] with 1:100 dilution of protease inhibitor cocktail III (Calbiochem). The tissue and 10 vol. of RIPA buffer were homogenized in a 2 ml glass homogenization tube with Teflon-coated homogenizer (20 up-and-down motions). The homogenate was transferred to a 1.5 ml microcentrifuge tube and centrifuged at 21100 ***g*** for 15 min at 4°C. The supernatant was removed from the pellet and the BCA (bicinchoninic acid) protein assay (Thermo-Pierce) was used to determine the protein concentration. Extracts were stored in aliquots at −80°C.

Hippocampal microdissection

Frozen brains were mounted on cryostat chucks with OCT (optimal cutting temperature) compound (Sakura Finetek USA) on dry ice, equilibrated to −22°C, and then sectioned with a cryostat at 200 μm. Sections with dorsal hippocampus (bregma −1.0 mm to bregma −2.3 mm, Figure 2A; Paxinos and Franklin, 2001) were mounted on Superfrost/Plus glass slides (Fisher Scientific) and a finger was placed underneath the section so that it would melt to the slide. Two or three sections were mounted on each slide and slides were stored at −80°C until microdissection.

Slides with sections were placed on a Petri dish with ice and observed under a Zeiss StemiDV4 stereoscope (Carl Zeiss Microscopy and Imaging). The sections were thawed and the stratum oriens, dentate gyrus and rest of hippocampus were dissected (Figure 2B); four to seven sections were dissected from each brain. The hippocampal subregions were sonicated for 3 s with a sonic dismembrator at setting 2 (Model 100, Fisher Scientific) in 40 μl of ice cold RIPA buffer containing 1:100 protease inhibitor cocktail III. The samples were then centrifuged at 21100 ***g*** for 5 min at 4°C to pellet any insoluble material and protein was measured by the BCA method. The supernatants were stored at −80°C.

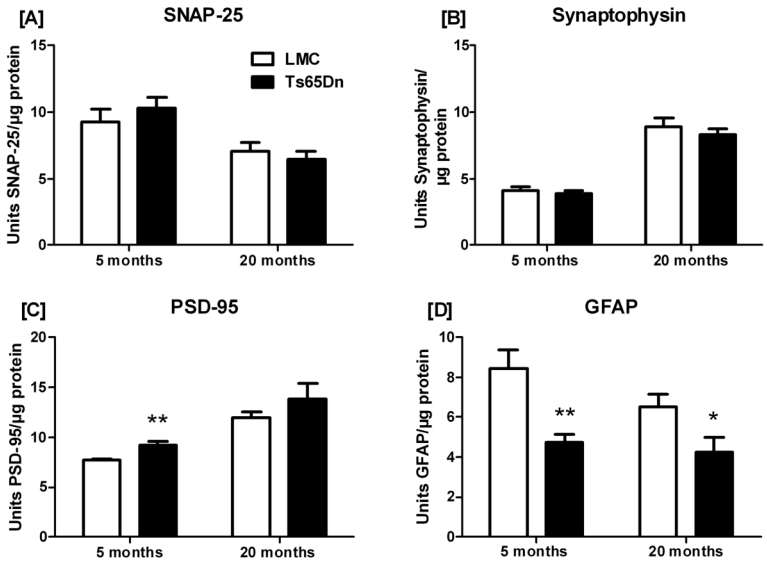

Figure 1 **Synaptic protein measurement in LMC and Ts65Dn hippocampal extracts**
The synaptic proteins SNAP-25 (**A**), synaptophysin (**B**), PSD-95 (**C**) and the astrocyte protein GFAP (**D**) were measured by ELISA in 5- and 20-month-old LMC and Ts65Dn hippocampal extracts. At 5 months of age, $n=7$ or 8 mice per genotype; at 20 months of age, $n=6$ mice for each genotype. For each ELISA, values for LMC and Ts65Dn hippocampus at the same age were compared with a Student's t test; $^{*}P<0.05$, $^{**}P<0.01$.

ELISA

Sandwich ELISAs for the presynaptic vesicular protein, synaptophysin, the presynaptic membrane protein SNAP-25 (25 kDa synaptosome-associated protein), the postsynaptic scaffolding protein PSD-95 (postsynaptic density 95), and GFAP (glial fibrillary acidic protein) were performed as described (Gottschall et al., 2010) with modifications to some capture and detection antibodies and dilutions (Table 1). The secondary antibody was goat anti-rabbit IgG conjugated to HRP (horseradish peroxidase) (Millipore) diluted 1:1000 (synaptophysin and PSD-95) or 1:5000 (SNAP-25 and GFAP). Supernatant from an RIPA homogenate of whole mouse brain was used for constructing a standard curve with a selected dilution (near beginning of saturation) designated as 100 units of binding activity (Gottschall et al., 2010). Levels of markers measured in units were normalized by dividing the units obtained in ELISA by the protein concentration for the sample to obtain units of ELISA protein per µg of protein.

Immunoblotting

Sample extracts containing equal protein amounts (5 µg for glutamine synthetase, 15 µg for brevican and fragments, and 30 µg for versican and fragments) were combined with 2 × Laemmli sample buffer, heated at 95 ℃ for 4 min, loaded on to Tris/glycine 4–20% gradient SDS/PAGE gels (Invitrogen) and electrophoresed. Proteins were electorphoretically transferred to PVDF (Immobilon, Millipore) and probed for various antigens. Membranes were washed in buffer B (1 × PBS and 0.05% Tween-20, pH 7.4) for 5 min and then blocked in buffer B containing 5% (w/v) non-fat dried skimmed milk powder (SaCo) for 1 h. Table 1 lists the primary antibodies and dilutions used; the antibodies referring to amino acid sequences are neoepitope metalloproteinase cleavage sequences in either brevican or versican (Mayer et al., 2005; Ajmo et al., 2010). Blots were then incubated with goat anti-mouse IgG or goat anti-rabbit IgG conjugated to HRP (Millipore) diluted 1:20,000. Antigens were visualized with the Immobilon Western Chemiluminscent HRP Substrate (Millipore) and the blots were exposed using a Kodak 4000 MM imager (Carestream Health) or to autoradiography film (Denville Scientific).

Quantification of immunoblots

The Kodak Molecular Imaging Software (Carestream Health) was used to measure the mean intensity of each antigen band as well as the background for each blot. For the glutamine synthetase blots, the film was scanned at 400 dpi with the Perfection V700 Photo scanner (Epson), converted into 8-bit greyscale, the background subtracted, the colour inverted, and the mean intensity for each band measured with ImageJ software. For each method the background was subtracted from each sample and this value was then divided by the mean intensity for GAPDH (glyceraldehyde-3-phosphate dehydrogenase) for the same blot to obtain normalized mean intensity. For each antigen LMC and Ts65Dn normalized mean intensity values were divided by the average mean intensity for all LMC samples to obtain the percentage of LMC.

Immunohistochemistry

Each fixed hemibrain was sequentially cryoprotected in 15% and 30% sucrose overnight at 4 ℃, mounted on a cryostat

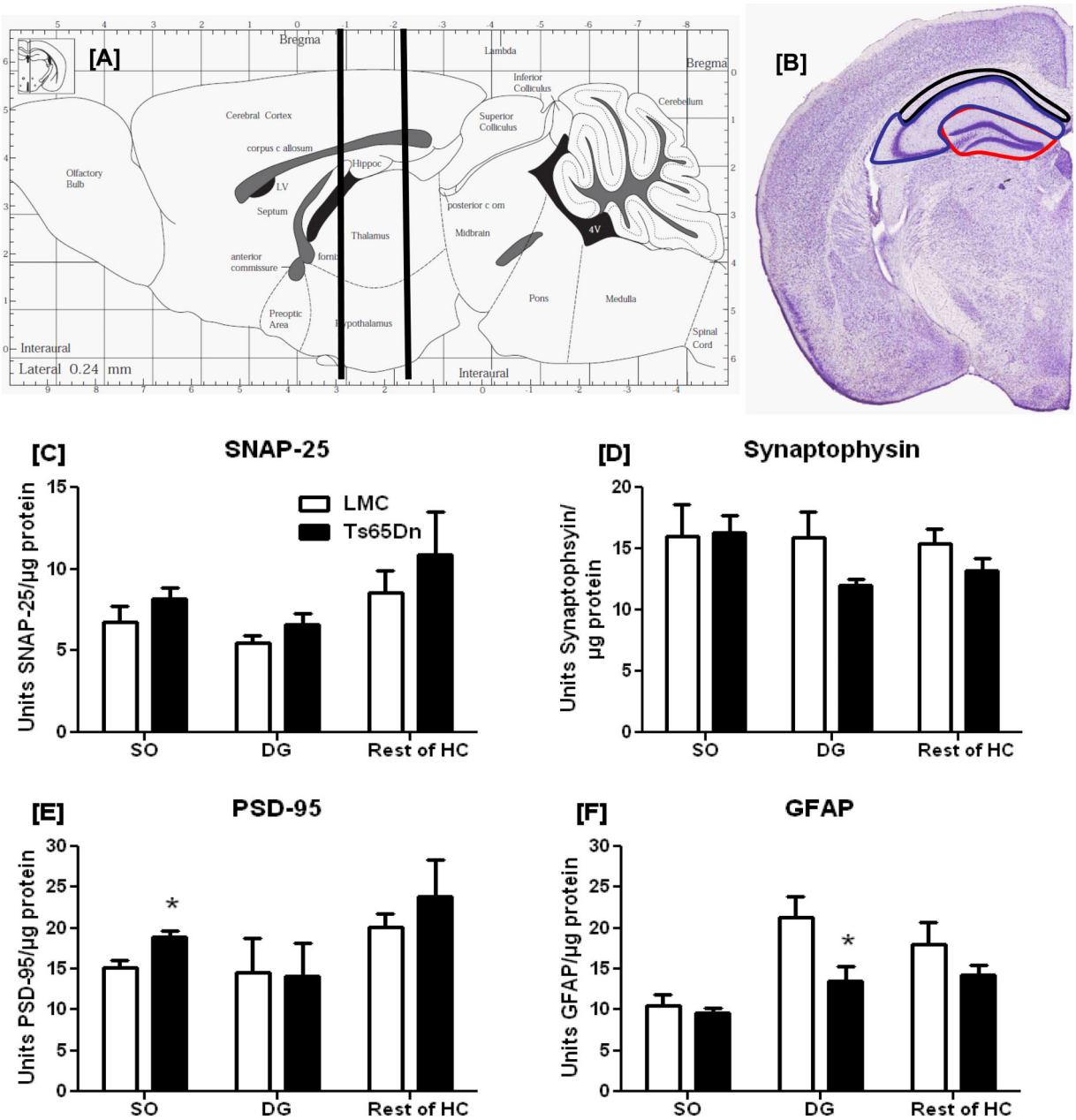

Figure 2 **Synaptic protein measurement in LMC and Ts65Dn hippocampal region extracts**
Hippocampal regions were microdissected from 200 µm hemibrain sections from 20 months old LMC and Ts65Dn mice between Bregma −1.0 mm to Bregma −2.3 mm (**A**; black lines indicate the boundaries of the sections) and SO (stratum oriens, black outline), DG (dentate gyrus, red outline) and remainder of the hippocampus (Rest of HC, blue outline) were microdissected (**B**). The synaptic proteins SNAP-25 (**C**), synaptophysin (**D**), PSD-95 (**E**) and astrocyte protein GFAP (**F**) were measured by ELISA ($n=5$ mice for each genotype). For each ELISA, values for LMC and Ts65Dn subregions were compared with a Student's t test; $^*P<0.05$. Images from (**A**) and (**B**) adapted from (Paxinos and Franklin, 2001).

chuck with OCT compound, equilibrated at −22°C, and sectioned at 30 µm with a Microm HM505 cryostat. Sections were stored free floating in PBS at 4°C until used in immunohistochemistry.

Three sections per brain bearing dorsal hippocampus were washed in PBS three times for 5 min each, blocked and permeabilized in 10% normal goat serum, 3% 1 M lysine, 0.3% Triton X-100 for 1 h and then incubated overnight at 4°C with biotinylated WFA (*Wisteria floribunda* agglutinin; 1:2000, Vector Laboratories) and rabbit anti-GFAP (1:2000, Dako). The sections were then washed and incubated at 1:1000 with streptavidin–Alexa Fluor® 488 and goat anti-rabbit IgG–Alexa Fluor® 568 (Millipore). Sections were mounted on Superfrost/Plus glass slides with Vectashield

Table 1 Antibodies used for ELISA and immunoblotting

Application	Antibody	Source	Dilution
ELISA capture	Mouse anti-SNAP-25	Millipore	1:200
	Mouse anti-synaptophysin	Millipore	1:200
	Mouse anti-PSD-95	NeuroMab	1:250
	Mouse anti-GFAP	Millipore	1:250
ELISA detection	Rabbit anti-SNAP-25	Sigma–Aldrich	1:1000
	Rabbit anti-synaptophysin	Santa Cruz	1:1000
	Rabbit anti-PSD-95	Millipore	4 μg/ml
	Rabbit anti-GFAP	Dako	1:1000
Western Blotting	Mouse anti-brevican	BD Biosciences	1:1000
	Rabbit anti-EAMESE	Gottschall Laboratory, Mayer et al. (2005)	1:1000
	Rabbit anti-SAHPSA	Ajmo et al. (2010)	1:500
	Mouse anti-versican V2 (12C5)	DSHB	1:1000
	Rabbit anti-NIVNSE	Gottschall Laboratory	1:500
	Mouse anti-glutamine synthetase	Millipore	1:5000
	Rabbit anti-GAPDH	Cell Signalling	1:5000

Mounting Medium with DAPI (4′,6-diamidino-2-phenylindole; Vector Laboratories).

Image acquisition and analysis

Images were acquired with an Olympus BX51 microscope using a ×20 PlanApo lens (Olympus Inc.) and Metamorph software (Molecular Devices) using the same gain and intensity. TIFF files were exported for analysis with ImageJ software. The polygon tool was used to draw a boundary around each PNN, and mean intensity and area were measured (at least 30 PNNs per mouse). The mean intensity was divided by area for each PNN and the quartiles determined. Each net was assigned a category as follows: 1 (<25th percentile), 2 (>25th percentile and <50th percentile), 3 (>50th percentile and <75th percentile) and 4 (>75th percentile). This same procedure was followed to categorize PNNs based on area. The experimenter was blinded to the genotype during image acquisition and analysis.

RNA isolation and qRT–PCR (quantitative reverse transcription–PCR)

Total RNA was isolated from 5 months old LMC and Ts65Dn whole hippocampus using the RNeasy Lipid Tissue Mini Kit (Qiagen). Total RNA concentration was determined with the NanoDrop ND-1000 Spectrophotometer (Thermo Scientific) and 1 μg of total RNA was reverse-transcribed with the High Capacity cDNA Reverse Transcription Kit (Applied Biosystems). qRT–PCR was performed using the ABI7900HT Fast Real-Time PCR System with TaqMan Gene Expression Master Mix and TaqMan Gene Expression Assays (Applied Biosystems) for the following genes: *Adamts1* (Assay ID Mm00477355_m1), *Adamts4* (Assay ID Mm00556068_m1), *Adamts5* (Assay ID Mm00478620_m1) and *Gapdh* (Assay ID Mm03302249_g1). Samples were assayed in triplicate and the average logarithmic C_t (threshold cycle) value was converted into the linear form using the conversion 2^{-Ct} (Nairn et al., 2007). For each sample, linear C_t values for the *Adamts* genes were divided by the linear C_t *Gapdh* value to obtain relative transcript abundance.

Statistics

Statistical analysis was performed with GraphPad Prism 5 (GraphPad Software). Data from RAWM were analysed with a repeated measures of ANOVA with Bonferroni pairwise comparison. We further compared the average number of errors made during each block by one-way ANOVA for each genotype followed by Bonferroni's multiple comparison test. ELISA, densitometry and relative transcript abundance data were analysed with Student's *t* test (two-tailed); PNN categorical data were analysed with the Cochran–Armitage test for trend; and values for PNN mean intensity/area and area were analysed with the Mann–Whitney *U* test. For all tests, $P<0.05$ was considered a significant difference. All values are shown as means ± S.E.M.

RESULTS

Measurement of synaptic proteins by ELISA

Our laboratory developed ELISAs for SNAP-25, synaptophysin and PSD-95 (Gottschall et al., 2010) and we used these to measure relative synaptic abundance in hippocampal extracts from LMC and Ts65Dn mice. We found no significant difference in the levels of the presynaptic markers SNAP-25 or synaptophysin at either 5 or 20 months of age in Ts65Dn whole hippocampus (Figures 1A and 1B) compared with LMC. However, a significant 19% increase in PSD-95 was observed at 5 but not 20 months of age in the Ts65Dn hippocampus (Figure 1C), although there was a trend for an increase at 20 months. Levels of the astrocyte intermediate filament GFAP were also measured and we found a 44% decrease at 5 months of age and a 35% decrease at 20 months of age in whole hippocampus compared with LMC extracts (Figure 1D). We saw no difference in the levels of these proteins in the frontal cortex and cerebellum at either 5 (Supplementary Figure S1 available at http://www.asnneuro.org/an/004/an004e073add.htm) or 20 months of age (Supplementary

Figure S2 available at http://www.asnneuro.org/an/004/an004e073add.htm) in the Ts65Dn mouse compared with LMC extracts.

Only a minimal difference in synapse abundance was observed in whole Ts65Dn hippocampal extracts; however, there may be regional, localized changes in synaptic markers that are masked by a variable baseline when assaying whole tissue extract. Thus, levels of synaptic markers were measured in microdissected hippocampus including stratum oriens, dentate gyrus and remainder of hippocampus (Figure 2B). We found a 24% increase in PSD-95 in Ts65Dn stratum oriens compared with LMCs (Figure 2E) with no changes in SNAP-25 and synaptophysin in any of the Ts65Dn hippocampal subregions compared with their LMCs (Figures 2C and 2D). The decrease in GFAP seen in the Ts65Dn whole hippocampal extract was markedly observed in the Ts65Dn dentate gyrus (Figure 2F), with a 37% decline compared with LMC dentate gyrus. To determine whether the decrease in GFAP in Ts65Dn whole hippocampus and hippocampal regions was consistent with another astrocyte-specific protein, we examined the level of glutamine synthesis by Western blotting, a protein involved in both GABA (γ-aminobutyric acid) and glutamate neurotransmission. At either 5 or 20 months old whole hippocampus and in hippocampal regions there was no difference in glutamine synthetase levels between Ts65Dn and LMC extracts (data not shown).

Spatial learning and memory in aged Ts65Dn and LMC mice

We next wanted to determine whether the decrease in PSD-95 abundance was associated with alteration in hippocampal-dependent, spatially mediated learning and memory by subjecting the 20-month-old mice to platform seeking in the RAWM (Alamed et al., 2006). Mice were tested over 3 days: day 1 was learning of the platform location, day 2 was recall and day 9 tested long-term recall of the platform location. Both Ts65Dn and LMC mice committed approximately five errors for the first block of three trials on day 1 (Figure 3). The LMC mice appeared to learn the location of the platform more quickly than Ts65Dn mice as they averaged 1.0 error on the last block (block 4) of day 1, while the Ts65Dn mice averaged 3.5 errors. On the second day of testing, the LMC mice averaged 1.9 errors for block 5, while the Ts65Dn mice averaged 4.3 errors (Figure 3). The Ts65Dn mice continued to commit more errors than the LMC mice over all trials on day 2 ending with 2.8 errors compared with 0.9 errors for LMC mice. This same trend was apparent on day 9; the LMC mice committed well less than 1 error over all four blocks, while the Ts65Dn mice reached a plateau at 2.5 errors per block (Figure 3). We found a significant genotype effect by repeated-measures ANOVA [$F(1,14)=12.07$, $P=0.0041$] as well as a significant difference between LMC and Ts65Dn mice for blocks 3 and 9 by Bonferroni pairwise comparison. Further, by block 3 and for all remaining blocks, the LMC mice made significantly fewer errors than during block 1 (Figure 3). However, there were no significant differences between the errors made in block 1 and all other blocks for the Ts65Dn mice. These results suggest that aged Ts65Dn mice exhibit impaired spatial learning and memory.

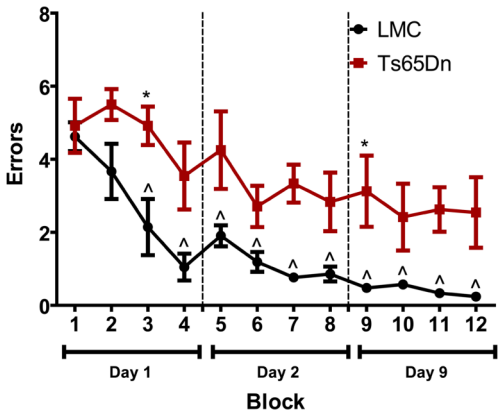

Figure 3 RAWM performance in aged LMC and Ts65Dn mice
20-month-old LMC and Ts65Dn mice ($n=7$ or 8 mice per genotype) received 12 RAWM trials (four blocks of three trials) for each day tested. Data were analysed with a two-way repeated measures ANOVA and Bonferroni pairwise comparison; *$P<0.05$ for Ts65Dn compared with LMC at the same time point. For each genotype, errors for blocks 2–12 were compared with errors from block 1 with a one-way ANOVA with Bonferroni pairwise comparison test; ^$P<0.01$.

Lectican abundance and processing in the Ts65Dn and LMC hippocampus

Lecticans are essential components of the ECM in the CNS and are thought to regulate structural and functional plasticity of synapses especially during critical periods late during development (Pizzorusso et al., 2002). Since the lectican-cleaving metalloproteinases, ADAMTS1 and ADAMTS5 are approximately 2-fold overexpressed in the Ts65Dn hippocampus (Supplementary Figure S3 available at http://www.asnneuro.org/an/004/an004e073add.htm), we hypothesized that there would be excess processing of lecticans in Ts65Dn brain that may relate to changes in synapse abundance. The abundance and ADAMTS processing of two prominent lecticans (brevican and versican) in the hippocampus were measured. Brevican content and processing were unchanged in 5 and 20 months old Ts65Dn whole hippocampus or in any of the 20 months old hippocampal subregions (data not shown). However, the abundance of versican V2, 245 kDa holoprotein, was increased significantly at both 5 months (56%) and 20 months (224%) of age in Ts65Dn hippocampus (Figure 4), but there was no change in the level of the ADAMTS-derived proteolytic fragment NIVNSE (50 kDa). In hippocampal subregions, there was a marked 250% increase in versican V2 abundance in the Ts65Dn stratum oriens compared with LMC. While there was also a trend towards an increase in both the dentate gyrus and rest of hippocampus (89%) this was not a statistically significant difference (Figure 5).

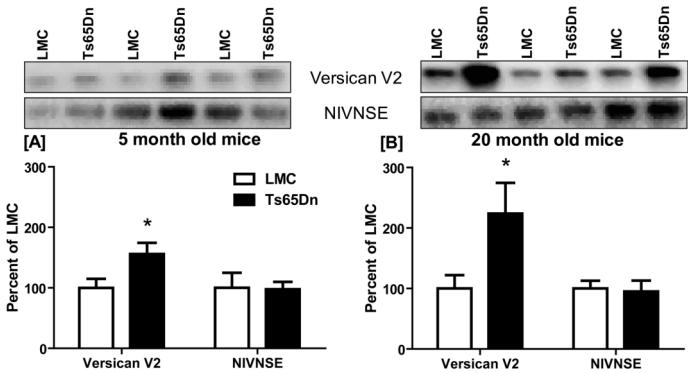

Figure 4 **Versican V2 abundance and processing in LMC and Ts65Dn hippocampal extracts**
Immunoblots of hippocampal extracts from mice at 5 months of age, $n=7$ mice per genotype; and mice at 20 months of age, $n=6$ mice per genotype. NIVNSE refers to the ADAMTS-derived N-terminal fragment of versican V2. Mean densitometric values were normalized to GAPDH (data not shown) and then expressed as a percentage of LMC. For each age, values for LMC and Ts65Dn hippocampus were compared with a Student's t test; $^*P<0.05$.

Correlation between versican V2 abundance and RAWM performance

Since spatial memory as measured in the RAWM is mediated by the hippocampus, and the presence of lecticans is important in synaptic plasticity (Frischknecht et al., 2009), we wanted to examine whether there was a correlation between altered abundance of versican V2 and performance in the RAWM. There was a correlation between increased versican and an increase in the number of errors in the final block (block 12) of the RAWM in the Ts65Dn stratum oriens ($P=0.0044$, $r^2=0.9912$), but not LMC stratum oriens (Figure 6A). Further, there was no correlation between versican abundance and errors in the final block of the RAWM in the Ts65Dn or LMC dentate gyrus or rest of hippocampus (Figures 6B and 6C).

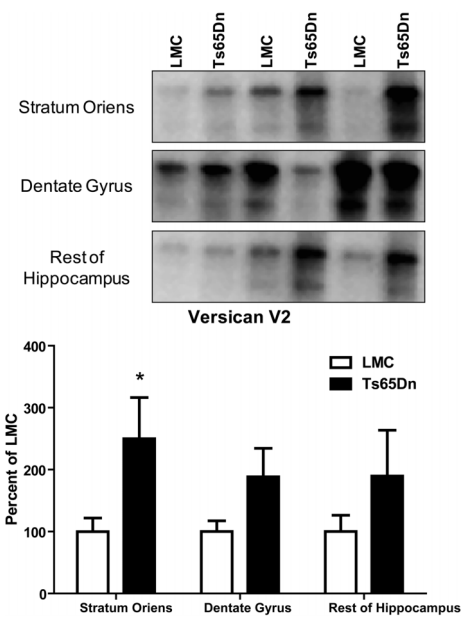

Figure 5 Versican V2 abundance in LMC and Ts65Dn hippocampal region extracts
Immunoblots from 20-month-old LMC and Ts65Dn hippocampal regions ($n=5$ mice for each genotype). The mean versican V2 densitometric value for each sample was normalized to GAPDH (data not shown) and then expressed as a percentage of LMC. For each hippocampal region, the LMC and Ts65Dn values were compared with a Student's t-test; $^*P<0.05$.

PNNs in stratum oriens

The increase in versican V2 in stratum oriens could be attributed to alterations in PNNs, of which versican V2 has been shown to be a component (Carulli et al., 2006; Deepa et al., 2006). PNNs were visualized with WFA, a lectin that binds to *N*-acetylgalactosamine residues (Figures 7A and 7B), and PNNs were categorized based on the mean intensity per area (category 1–4, with 1 being the lowest values). There were more Ts65Dn PNNs in category 1 and fewer in category 4 compared with LMCs (Figure 7C; $\chi^2=3.922$, df=1, $P=0.0476$) and an overall 21% decline in mean intensity/area (Figure 7D). This decrease could be due to an increase in PNN area so PNNs were also classified by area into categories as above. There was a greater number of Ts65Dn PNNs of the highest area (category 4) and lower number in the smallest area (category 1) compared with LMCs (Figure 7E; $\chi^2=7.265$, df=1, $P=0.0070$). Indeed, Ts65Dn PNNs exhibited a 24% increase in area compared with LMCs (Figure 7F). These data suggest that Ts65Dn stratum oriens PNNs encompass a larger neuronal surface than seen with LMC PNNs.

DISCUSSION

Decreased numbers of presynaptic and postsynaptic terminals were previously observed during development in Ts65Dn stratum oriens (Chakrabarti et al., 2007) and Ts65Dn dentate gyrus has been shown to have a reduced number of neurons (Insausti et al., 1998) and deficient LTP (Kleschevnikov et al.,

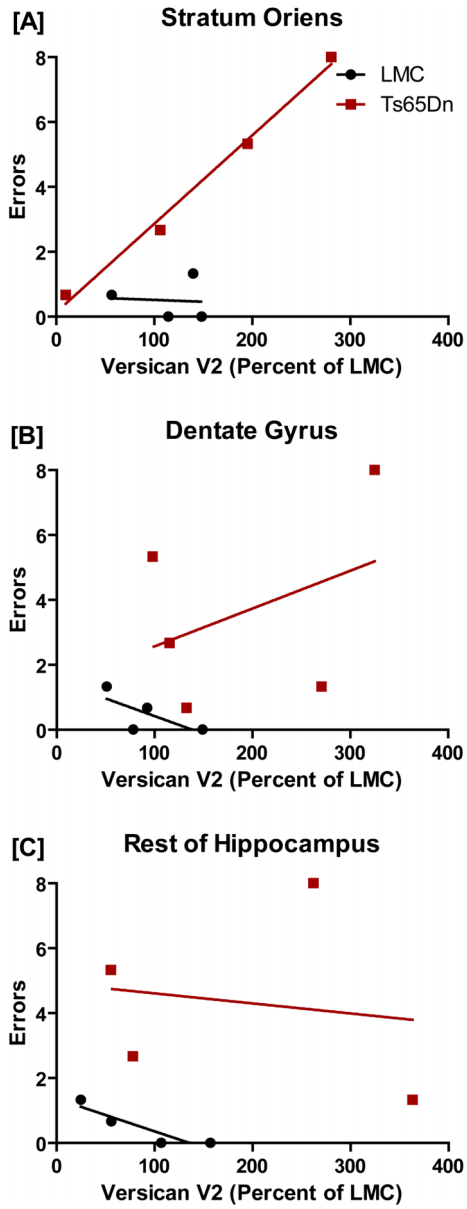

Figure 6 Correlation analysis between versican V2 in hippocampal region extracts and RAWM performance for LMC and Ts65Dn mice
Correlation between versican V2 immunoreactivity and the number of errors committed in the final block (block 12) of the RAWM for stratum oriens (**A**), dentate gyrus (**B**), and rest of hippocampus (**C**). Linear regression analysis was performed to determine the significance of the r^2 value (see the text).

2004). By undertaking hippocampal microdissection, we found that aged Ts65Dn mice exhibit an increase in levels of PSD-95, PNNs that encompass greater neuronal surface areas and a marked increase in levels of versican V2 in hippocampal stratum oriens. With this microdissection technique, we were able to measure synaptic markers and ECM proteins and found localized changes that may be masked when measured in whole brain tissue. Further, there appeared to be an association between the localized, increased levels of ECM and learning and memory deficits in the Ts65Dn mouse.

While it is known that trisomy of human chromosome 21 leads to DS, the exact genes and molecular mechanism(s) underlying the cognitive impairment are poorly understood. Initially, we tested whether overexpression of the gene *Adamts1*, encoding a metalloproteinase that cleaves lecticans in the ECM of the CNS, and capable of altering neural plasticity, may be involved in the pathophysiology of mental retardation in DS. Our data with the Ts65Dn mouse, however, suggest that this is not the case. While we found a 2-fold up-regulation in *Adamts1* in the Ts65Dn hippocampus, this change was not as robust as that seen in adult DS brains, and we found no changes in the ADAMTS-specific cleavage fragments of the lecticans brevican and versican. However, intact versican V2 holoprotein was found to be significantly elevated in the Ts65Dn hippocampus, a finding that could implicate changes in the ECM as associated with the cognitive deficit in the Ts65Dn mouse.

Versican occurs as three isoforms in the brain (V0–V2), with V2 the primary isoform found in adult brain (Milev et al., 1998). V2 has been shown to inhibit neurite outgrowth whether bearing CS chains or not (Schmalfeldt et al., 2000). Versican V2 abundance was increased in Ts65Dn hippocampus and stratum oriens with a trend towards an increase in dentate gyrus and remainder of the hippocampus. Further, we found a significant positive correlation between versican V2 in Ts65Dn stratum oriens and the number of errors made in the final block of the RAWM. We found a range in the abundance of versican V2 immunoreactivity in Ts65Dn mice that was not observed with brevican. This variability is directly associated with synaptic marker abundance in stratum oriens, suggesting it may be associated with the cognitive deficit in Ts65Dn mice.

We found a significant increase in PSD-95 at 5 months (19%) but not at 20 months of age in Ts65Dn whole hippocampus. However, there was a significant 24% increase in Ts65Dn stratum oriens at 20 months of age. Previous studies that have measured synaptic proteins in the Ts65Dn brain have yielded conflicting results. Using synaptosomes from whole cortex of Ts65Dn mice, one study showed no change in multiple synaptic markers (Fernandez et al., 2009). Since the changes observed here were localized to stratum oriens, these changes may have been masked in previous studies that examined large brain regions. Another study that measured synaptophysin in stratum oriens found increased levels in Ts65Dn mice at 6 months of age, but these levels were not different at 16 months of age (Belichenko et al., 2004). Since we found no changes in presynaptic synaptic protein levels, it may be that there is no change in the number of synapses in this region, but rather an increase in the synapse size.

Stratum oriens contains multiple populations of inhibitory interneurons and an age-related loss of GAD67-positive inhibitory interneurons has been observed in rats (Stanley et al., 2012). This same age-dependent decrease in interneurons may not occur in Ts65Dn stratum oriens. One study showed pharamacological antagonism of $GABA_A$ receptors rescued the LTP deficit in Ts65Dn mice which suggests either increased GABA-mediated inhibition or an increase in plasticity

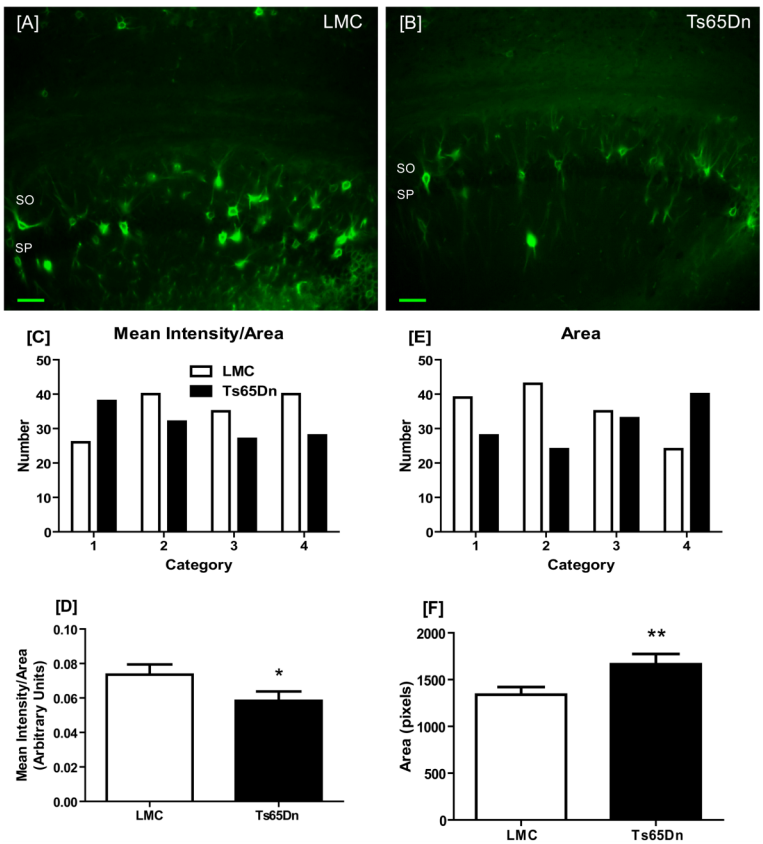

Figure 7 **PNNs in LMC and Ts65Dn stratum oriens**

Representative images of WFA-positive PNNs in LMC (**A**) and Ts65Dn (**B**) SO (stratum oriens) and SP (stratum pyramidale). Individual PNNs were measured and the mean intensity and area determined ($n=141$ LMC PNNs and $n=125$ Ts65Dn PNNs). PNNs were then categorized based on their mean intensity per area (**C**). Note that category 1 indicates the lowest mean intensity/area. Mean intensity/area values for measured PNNs were also compared (**D**). PNNs were also categorized by area (**E**; category 1 is smallest area) and the values for area of PNNs was compared (**F**). (**C**) and (**E**) were analysed with Cochran–Armitage test for trend (see the text for details). *$P<0.05$ and **$P<0.01$ by Mann–Whitney U test. (**A**, **B**) Scale bar: 100 μm.

at GABAergic synapses (Costa and Grybko, 2005). Anti-Hebbian LTP or LTP that occurs when presynaptic firing is paired with postsynaptic hyperpolarization, has been reported at excitatory boutons that synapse on inhibitory interneurons in the stratum oriens (Lamsa et al., 2007). The excitatory synapses of Ts65Dn stratum oriens interneurons could undergo this plasticity to a greater extent than in LMC mice to promote a stronger, larger synapse. Indeed, local changes in protein synthesis, including PSD-95, serve to stabilize potentiated synapses (Ostroff et al., 2002). This change would increase excitation of the inhibitory interneurons and stimulate inhibitory neurotransmission in the hippocampus. This plasticity may occur early in development, denoted by the increase in PSD-95 observed at 5 months with the stronger synapses maintained throughout aging.

The strengthened interneurons in Ts65Dn stratum oriens could be maintained by the increased versican V2 which may represent an increase in PNNs. PNNs have been observed in stratum oriens (Mayer et al., 2005) and versican can be a component of PNNs, although the exact lectican composition of PNNs is not known. PNN formation can also be activity dependent (Zaremba et al., 1989; Dityatev et al., 2007), so stronger excitation of the interneurons may result in increased PNN formation and/or increased versican V2 in existing PNNs surrounding inhibitory interneurons. Indeed, our data indicate increased PNN surface area on neurites in Ts65Dn stratum oriens which could stabilize inhibitory interneurons and presumably increase inhibitory output leading to deficient spatial learning and memory.

The decrease in GFAP in both 5- and 20-month-old Ts65Dn hippocampus could indicate a decrease in the number or reactivity of astrocytes. Studies have reported increased S-100 immunoreactive cells throughout development and aging in DS temporal cortex (Griffin et al., 1989) and also an increase in S-100-positive cells in the DS hippocampus from gestation to old age (Mito and Becker, 1993), but also no difference in S-100 cell distribution in DS brain (Michetti et al., 1990). Interestingly, expression of *Gfap* was found to be significantly lower in the neocortex of DS patients (Goodison et al., 1993). Additionally, modest increases in GFAP immunoreactive astrocytes (Holtzman et al., 1996) and GFAP by immunoblotting (Contestabile et al., 2006) have

been reported in the Ts65Dn hippocampus. We found the GFAP decrease was localized to the Ts65Dn dentate gyrus, an area that has been associated with deficient LTP (Kleschevnikov et al., 2004). A recent study demonstrated that astrocytic gliosis (accompanied with an increased in GFAP) was associated with a decrease in neuronal inhibition (Ortinski et al., 2010). Decreased inhibition was related to a decrease in glutamine synthetase, the enzyme that converts glutamate to glutamine and ultimately to GABA in inhibitory terminals. Glutamine synthetase activity was shown to be elevated in 19-month-old Ts65Dn hippocampus which would support an increase in inhibition (Contestabile et al., 2006). While we found no difference in glutamine synthetase between LMC and Ts65Dn hippocampus, it is possible there is a change in activity beyond protein levels. Thus, it is possible that a decrease in GFAP may indeed be associated with an increase in neuronal inhibition which would support the decrease in LTP in the Ts65Dn dentate gyrus.

In summary, we have found that aged Ts65Dn mice exhibit deficient hippocampal-dependent spatial learning and memory accompanied by a modest increase in PSD-95 and a marked increase in versican V2 in hippocampal stratum oriens. Further, the increase in versican V2 correlated with increased number of errors in the RAWM, a measure of spatial learning and memory. These molecular changes in the composition of the ECM may functionally influence the cognitive deficit in the Ts65Dn mouse and in DS patients.

ACKNOWLEDGEMENTS

We acknowledge Brenda Gannon for technical assistance, Drs Marcia Gordon and Dave Morgan (Byrd Alzheimer Institute, University of South Florida, Tampa, FL, U.S.A.) for insight and assistance with the RAWM, and Dr Galen Wenger (UAMS). We also acknowledge the Imaging Core of the Neuroscience Research Center Core Facility at UAMS [P30NS047546] for the use of the Olympus microscope and Dr Steve Post for allowing the use of the Kodak 4000MM Imager. The 12C5 antibody developed by Richard A. Asher was obtained from the Developmental Studies Hybridoma Bank developed under the auspices of the National Institute of Child Health and Human Development and maintained at The University of Iowa, Department of Biology, Iowa City, IA, U.S.A.

FUNDING

This work was supported, in part, by the National Institute on Aging [grant number R01 AG022101].

REFERENCES

Ajmo JM, Bailey LA, Howell MD, Cortez LK, Pennypacker KR, Mehta HN, Morgan D, Gordon MN, Gottschall PE (2010) Abnormal post-translational and extracellular processing of brevican in plaque-bearing mice over-expressing APPsw. J Neurochem 113:784–795.

Alamed J, Wilcock DM, Diamond DM, Gordon MN, Morgan D (2006) Two-day radial-arm water maze learning and memory task; robust resolution of amyloid-related memory deficits in transgenic mice. Nat Protoc 1:1671–1679.

Belichenko NP, Belichenko PV, Kleschevnikov AM, Salehi A, Reeves RH, Mobley WC (2009a) The 'Down syndrome critical region' is sufficient in the mouse model to confer behavioral, neurophysiological, and synaptic phenotypes characteristic of Down syndrome. J Neurosci 29:5938–5948.

Belichenko PV, Masliah E, Kleschevnikov AM, Villar AJ, Epstein CJ, Salehi A, Mobley WC (2004) Synaptic structural abnormalities in the Ts65Dn mouse model of Down syndrome. J Comp Neurol 480:281–298.

Belichenko PV, Kleschevnikov AM, Salehi A, Epstein CJ, Mobley WC (2007) Synaptic and cognitive abnormalities in mouse models of Down syndrome: exploring genotype-phenotype relationships. J Comp Neurol 504:329–345.

Belichenko PV, Kleschevnikov AM, Masliah E, Wu C, Takimoto-Kimura R, Salehi A, Mobley WC (2009b) Excitatory–inhibitory relationship in the fascia dentata in the Ts65Dn mouse model of Down syndrome. J Comp Neurol 512:453–466.

Bruckner G, Brauer K, Hartig W, Wolff JR, Rickmann MJ, Derouiche A, Delpech B, Girard N, Oertel WH, Reichenbach A (1993) Perineuronal nets provide a polyanionic, glia-associated form of microenvironment around certain neurons in many parts of the rat brain. Glia 8:183–200.

Burger PC, Vogel FS (1973) The development of the pathologic changes of Alzheimer's disease and senile dementia in patients with Down's syndrome. Am J Pathol 73:457–476.

Canfield MA, Honein MA, Yuskiv N, Xing J, Mai CT, Collins JS, Devine O, Petrini J, Ramadhani TA, Hobbs CA et al. (2006) National estimates and race/ethnic-specific variation of selected birth defects in the United States, 1999–2001. Birth Defects Res A Clin Mol Teratol 76:747–756.

Carulli D, Rhodes KE, Brown DJ, Bonnert TP, Pollack SJ, Oliver K, Strata P, Fawcett JW (2006) Composition of perineuronal nets in the adult rat cerebellum and the cellular origin of their components. J Comp Neurol 494:559–577.

Chakrabarti L, Galdzicki Z, Haydar TF (2007) Defects in embryonic neurogenesis and initial synapse formation in the forebrain of the Ts65Dn mouse model of Down syndrome. J Neurosci 27:11483–11495.

Contestabile A, Fila T, Bartesaghi R, Ciani E (2006) Choline acetyltransferase activity at different ages in brain of Ts65Dn mice, an animal model for Down's syndrome and related neurodegenerative diseases. J Neurochem 97:515–526.

Cooper JD, Salehi A, Delcroix JD, Howe CL, Belichenko PV, Chua-Couzens J, Kilbridge JF, Carlson EJ, Epstein CJ, Mobley WC (2001) Failed retrograde transport of NGF in a mouse model of Down's syndrome: reversal of cholinergic neurodegenerative phenotypes following NGF infusion. Proc Natl Acad Sci USA 98:10439–10444.

Costa AC, Grybko MJ (2005) Deficits in hippocampal CA1 LTP induced by TBS but not HFS in the Ts65Dn mouse: a model of Down syndrome. Neurosci Lett 382:317–322.

Davisson MT, Schmidt C, Akeson EC (1990) Segmental trisomy of murine chromosome 16: a new model system for studying Down syndrome. Prog Clin Biol Res 360:263–280.

Deepa SS, Carulli D, Galtrey C, Rhodes K, Fukuda J, Mikami T, Sugahara K, Fawcett JW (2006) Composition of perineuronal net extracellular matrix in rat brain: a different disaccharide composition for the net-associated proteoglycans. J Biol Chem 281:17789–17800.

Demas GE, Nelson RJ, Krueger BK, Yarowsky PJ (1996) Spatial memory deficits in segmental trisomic Ts65Dn mice. Behav Brain Res 82:85–92.

Demas GE, Nelson RJ, Krueger BK, Yarowsky PJ (1998) Impaired spatial working and reference memory in segmental trisomy (Ts65Dn) mice. Behav Brain Res 90:199–201.

Dityatev A, Bruckner G, Dityateva G, Grosche J, Kleene R, Schachner M (2007) Activity-dependent formation and functions of chondroitin sulfate-rich extracellular matrix of perineuronal nets. Dev Neurobiol 67:570–588.

Epstein CJ (2002) 2001 William Allan Award Address. From Down syndrome to the 'human' in 'human genetics'. Am J Hum Genet 70:300–313.

Escorihuela RM, Vallina IF, Martinez-Cue C, Baamonde C, Dierssen M, Tobena A, Florez J, Fernandez-Teruel A (1998) Impaired short- and long-term memory in Ts65Dn mice, a model for Down syndrome. Neurosci Lett 247:171–174.

Fernandez F, Trinidad JC, Blank M, Feng DD, Burlingame AL, Garner CC (2009) Normal protein composition of synapses in Ts65Dn mice: a mouse model of Down syndrome. J Neurochem 110:157–169.

Frischknecht R, Heine M, Perrais D, Seidenbecher CI, Choquet D, Gundelfinger ED (2009) Brain extracellular matrix affects AMPA receptor lateral mobility and short-term synaptic plasticity. Nat Neurosci 12:897–904.

Galtrey CM, Fawcett JW (2007) The role of chondroitin sulfate proteoglycans in regeneration and plasticity in the central nervous system. Brain Res Rev 54:1–18.
Goodison KL, Parhad IM, White CL, 3rd, Sima AA, Clark AW (1993) Neuronal and glial gene expression in neocortex of Down's syndrome and Alzheimer's disease. J Neuropathol Exp Neurol 52:192–198.
Gottschall PE, Ajmo JM, Eakin AK, Howell MD, Mehta H, Bailey LA (2010) Panel of synaptic protein ELISAs for evaluating neurological phenotype. Exp Brain Res 201:885–893.
Griffin WS, Stanley LC, Ling C, White L, MacLeod V, Perrot LJ, White III CL, Araoz C (1989) Brain interleukin 1 and S-100 immunoreactivity are elevated in Down syndrome and Alzheimer disease. Proc Natl Acad Sci USA 86:7611–7615.
Hamel MG, Ajmo JM, Leonardo CC, Zuo F, Sandy JD, Gottschall PE (2008) Multimodal signaling by the ADAMTSs (a disintegrin and metalloproteinase with thrombospondin motifs) promotes neurite extension. Exp Neurol 210:428–440.
Holtzman DM, Santucci D, Kilbridge J, Chua-Couzens J, Fontana DJ, Daniels SE, Johnson RM, Chen K, Sun Y, Carlson E, Alleva E, Epstein CJ, Mobley WC (1996) Developmental abnormalities and age-related neurodegeneration in a mouse model of Down syndrome. Proc Natl Acad Sci USA 93:13333–13338.
Hunter CL, Bimonte HA, Granholm AC (2003) Behavioral comparison of 4 and 6 month-old Ts65Dn mice: age-related impairments in working and reference memory. Behav Brain Res 138:121–131.
Hyde LA, Frisone DF, Crnic LS (2001) Ts65Dn mice, a model for Down syndrome, have deficits in context discrimination learning suggesting impaired hippocampal function. Behav Brain Res 118:53–60.
Insausti AM, Megias M, Crespo D, Cruz-Orive LM, Dierssen M, Vallina IF, Insausti R, Florez J (1998) Hippocampal volume and neuronal number in Ts65Dn mice: a murine model of Down syndrome. Neurosci Lett 253:175–178.
Isacson O, Seo H, Lin L, Albeck D, Granholm AC (2002) Alzheimer's disease and Down's syndrome: roles of APP, trophic factors and ACh. Trends Neurosci 25:79–84.
Jones GC, Riley GP (2005) ADAMTS proteinases: a multi-domain, multi-functional family with roles in extracellular matrix turnover and arthritis. Arthritis Res Ther 7:160–169.
Kern DS, Maclean KN, Jiang H, Synder EY, Sladek JR, Jr., Bjugstad KB (2011) Neural stem cells reduce hippocampal tau and reelin accumulation in aged Ts65Dn Down syndrome mice. Cell Transplant 20:371–379.
Kleschevnikov AM, Belichenko PV, Villar AJ, Epstein CJ, Malenka RC, Mobley WC (2004) Hippocampal long-term potentiation suppressed by increased inhibition in the Ts65Dn mouse, a genetic model of Down syndrome. J Neurosci 24:8153–8160.
Kuo H, Ingram DK, Walker LC, Tian M, Hengemihle JM, Jucker M (1996) Similarities in the age-related hippocampal deposition of periodic acid-Schiff-positive granules in the senescence-accelerated mouse P8 and C57BL/6 mouse strains. Neuroscience 74:733–740.
Kurt MA, Davies DC, Kidd M, Dierssen M, Florez J (2000) Synaptic deficit in the temporal cortex of partial trisomy 16 (Ts65Dn) mice. Brain Res 858:191–197.
Lamsa KP, Heeroma JH, Somogyi P, Rusakov DA, Kullmann DM (2007) Anti-Hebbian long-term potentiation in the hippocampal feedback inhibitory circuit. Science 315:1262–1266.
Lockstone HE, Harris LW, Swatton JE, Wayland MT, Holland AJ, Bahn S (2007) Gene expression profiling in the adult Down syndrome brain. Genomics 90:647–660.
Mayer J, Hamel MG, Gottschall PE (2005) Evidence for proteolytic cleavage of brevican by the ADAMTSs in the dentate gyrus after excitotoxic lesion of the mouse entorhinal cortex. BMC Neurosci 6:52.
Michetti F, Larocca LM, Rinelli A, Lauriola L (1990) Immunocytochemical distribution of S-100 protein in patients with Down's syndrome. Acta Neuropathol 80:475–478.
Milev P, Maurel P, Chiba A, Mevissen M, Popp S, Yamaguchi Y, Margolis RK, Margolis RU (1998) Differential regulation of expression of hyaluronan-binding proteoglycans in developing brain: aggrecan, versican, neurocan, and brevican. Biochem Biophys Res Commun 247:207–212.
Mito T, Becker LE (1993) Developmental changes of S-100 protein and glial fibrillary acidic protein in the brain in Down syndrome. Exp Neurol 120:170–176.
Mitsuno S, Takahashi M, Gondo T, Hoshii Y, Hanai N, Ishihara T, Yamada M (1999) Immunohistochemical, conventional and immunoelectron microscopical characteristics of periodic acid-Schiff-positive granules in the mouse brain. Acta Neuropathol 98:31–38.
Nairn AV, Kinoshita-Toyoda A, Toyoda H, Xie J, Harris K, Dalton S, Kulik M, Pierce JM, Toida T, Moremen KW et al. (2007) Glycomics of proteoglycan biosynthesis in murine embryonic stem cell differentiation. J Proteome Res 6:4374–4387.
Nelson L, Johnson JK, Freedman M, Lott I, Groot J, Chang M, Milgram NW, Head E (2005) Learning and memory as a function of age in Down syndrome: a study using animal-based tasks. Prog Neuropsychopharmacol Biol Psychiatry 29:443–453.
Olson LE, Roper RJ, Baxter LL, Carlson EJ, Epstein CJ, Reeves RH (2004) Down syndrome mouse models Ts65Dn, Ts1Cje, and Ms1Cje/Ts65Dn exhibit variable severity of cerebellar phenotypes. Dev Dyn 230:581–589.
Ortinski PI, Dong J, Mungenast A, Yue C, Takano H, Watson DJ, Haydon PG, Coulter DA (2010) Selective induction of astrocytic gliosis generates deficits in neuronal inhibition. Nat Neurosci 13:584–591.
Ostroff LE, Fiala JC, Allwardt B, Harris KM (2002) Polyribosomes redistribute from dendritic shafts into spines with enlarged synapses during LTP in developing rat hippocampal slices. Neuron 35:535–545.
Paxinos G, Franklin KBJ (2001) The Mouse Brain in Stereotaxic Coordinates, Second Edition. San Diego: Academic Press.
Pizzorusso T, Medini P, Berardi N, Chierzi S, Fawcett JW, Maffei L (2002) Reactivation of ocular dominance plasticity in the adult visual cortex. Science 298:1248–1251.
Pollonini G, Gao V, Rabe A, Palminiello S, Albertini G, Alberini CM (2008) Abnormal expression of synaptic proteins and neurotrophin-3 in the Down syndrome mouse model Ts65Dn. Neuroscience 156:99–106.
Popov VI, Kleschevnikov AM, Klimenko OA, Stewart MG, Belichenko PV (2011) Three-dimensional synaptic ultrastructure in the dentate gyrus and hippocampal area CA3 in the Ts65Dn mouse model of down syndrome. J Comp Neurol 519:1338–1354.
Porter S, Clark IM, Kevorkian L, Edwards DR (2005) The ADAMTS metalloproteinases. Biochem J 386:15–27.
Rauch U (2007) Brain matrix: structure, turnover and necessity. Biochem Soc Trans 35:656–660.
Reeves RH, Irving NG, Moran TH, Wohn A, Kitt C, Sisodia SS, Schmidt C, Bronson RT, Davisson MT (1995) A mouse model for Down syndrome exhibits learning and behaviour deficits. Nat Genet 11:177–184.
Salehi A, Faizi M, Colas D, Valletta J, Laguna J, Takimoto-Kimura R, Kleschevnikov A, Wagner SL, Aisen P, Shamloo M et al. (2009) Restoration of norepinephrine-modulated contextual memory in a mouse model of Down syndrome. Sci Transl Med 1:7ra17.
Schmalfeldt M, Bandtlow CE, Dours-Zimmermann MT, Winterhalter KH, Zimmermann DR (2000) Brain derived versican V2 is a potent inhibitor of axonal growth. J Cell Sci 113:807–816.
Siarey RJ, Stoll J, Rapoport SI, Galdzicki Z (1997) Altered long-term potentiation in the young and old Ts65Dn mouse, a model for Down Syndrome. Neuropharmacology 36:1549–1554.
Siarey RJ, Carlson EJ, Epstein CJ, Balbo A, Rapoport SI, Galdzicki Z (1999) Increased synaptic depression in the Ts65Dn mouse, a model for mental retardation in Down syndrome. Neuropharmacology 38:1917–1920.
Stanley EM, Fadel JR, Mott DD (2012) Interneuron loss reduces dendritic inhibition and GABA release in hippocampus of aged rats. Neurobiol Aging 33:431.e1–13.
Thase ME, Tigner R, Smeltzer DJ, Liss L (1984) Age-related neuropsychological deficits in Down's syndrome. Biol Psychiatry 19:571–585.
Yamaguchi Y (2000) Lecticans: organizers of the brain extracellular matrix. Cell Mol Life Sci 57:276–289.
Yuan W, Matthews RT, Sandy JD, Gottschall PE (2002) Association between protease-specific proteolytic cleavage of brevican and synaptic loss in the dentate gyrus of kainate-treated rats. Neuroscience 114:1091–1101.
Zaremba S, Guimaraes A, Kalb RG, Hockfield S (1989) Characterization of an activity-dependent, neuronal surface proteoglycan identified with monoclonal antibody Cat-301. Neuron 2:1207–1219.
Zimmermann DR, Dours-Zimmermann MT (2008) Extracellular matrix of the central nervous system: from neglect to challenge. Histochem Cell Biol 130:635–653.

Received 3 November 2011/14 December 2011; accepted 16 December 2011
Published as Immediate Publication 6 January 2012, doi 10.1042/AN20110037